# Analysis of Leaf Area Index and Fraction of PAR Absorbed by Vegetation Products From the Terra MODIS Sensor: 2000–2005

Wenze Yang, Dong Huang, Bin Tan, Julienne C. Stroeve, Nikolay V. Shabanov, Yuri Knyazikhin, Ramakrishna R. Nemani, and Ranga B. Myneni

***Abstract*—The analysis of two years of Collection 3 and five years of Collection 4 Terra Moderate Resolution Imaging Spectroradiometer (MODIS) Leaf Area Index (LAI) and Fraction of Photosynthetically Active Radiation (FPAR) data sets is presented in this article with the goal of understanding product quality with respect to version (Collection 3 versus 4), algorithm (main versus backup), snow (snow-free versus snow on the ground), and cloud (cloud-free versus cloudy) conditions. Retrievals from the main radiative transfer algorithm increased from 55% in Collection 3 to 67% in Collection 4 due to algorithm refinements and improved inputs. Anomalously high LAI/FPAR values observed in Collection 3 product in some vegetation types were corrected in Collection 4. The problem of reflectance saturation and too few main algorithm retrievals in broadleaf forests persisted in Collection 4. The spurious seasonality in needleleaf LAI/FPAR fields was traced to fewer reliable input data and retrievals during the boreal winter period. About 97% of the snow covered pixels were processed by the backup Normalized Difference Vegetation Index-based algorithm. Similarly, a majority of retrievals under cloudy conditions were obtained from the backup algorithm. For these reasons, the users are advised to consult the quality flags accompanying the LAI and FPAR product.**

***Index Terms*—Evaluation and assessment, Fraction of Photosynthetically Active Radiation (FPAR) absorbed by vegetation, Leaf Area Index (LAI), Moderate Resolution Imaging Spectroradiometer (MODIS).**

## I. Introduction

THE MODERATE resolution Imaging Spectroradiometer (MODIS) is an instrument on board NASA's Terra and Aqua platforms for remote sensing of the Earth's atmosphere, oceans and land surface. The Terra platform was launched on December 18, 1999 and the Aqua platform on May 4, 2002. The MODIS instrument has a swath width of 2 330 km, orbit height of 705 km, and produces global coverage every one to two days. MODIS measures reflected solar and emitted thermal radiation in 36 spectral bands and at three different spatial resolutions (250, 500, and 1000 m) [1].

The MODIS Land team is responsible for the development of algorithms for operationally producing 16 geophysical data products and their validation. The products include vegetation green leaf area index (LAI) and the fraction of photosynthetically active radiation (400–700 nm) absorbed by vegetation (FPAR) [2]. LAI is defined as the one-sided green leaf area per unit ground area in broadleaf canopies and as half the total needle surface area per unit ground area in coniferous canopies. These products are useful in studies of the exchange of fluxes of energy, mass (e.g., water and $CO_2$), and momentum between the surface and atmosphere [3].

Research on MODIS LAI and FPAR products is performed along three broad fronts—algorithm development, product analysis, and validation. Algorithm development includes the development of the at-launch algorithm [4]–[7], prototyping of the algorithm [8], and algorithm refinement [9]. Product analysis includes assessment of algorithm performance (this article) and product quality with emphasis on understanding how input data uncertainties constrain LAI/FPAR retrievals [10], [11]. Validation includes comparison of the product to field measurements scaled to MODIS resolution with the goal of quantitatively establishing product accuracy, precision, and uncertainty [12]–[18]. An article summarizing the validation activities of our team is included in this journal issue [19].

MODIS product versions are called Collections. Collection 3 is the first significant processing of MODIS data into products and covered the 26 month period from November 2000 to December 2002 (96 data sets, one for every eight-day period, totaling 157 GB). Collection 4 represents the latest version of MODIS products and contains the entire time series of data starting from February 2000 to the present (242 data sets, one for every eight-day period, totaling 396 GB). At 1-km spatial resolution, the land area constitutes about 170 million pixels, of which 128 million are vegetated. This article is based on analysis of the entire Collection 3 and 4 Terra MODIS LAI and FPAR data sets—about 108 billion pixel values. The purpose of the study is to compare the effects of version (Collection 3 versus 4), input reflectance data quality indirectly through the algorithm (main versus backup), snow (snow-free versus snow on the ground), and cloud (cloud-free versus cloudy) conditions on LAI/FPAR retrievals.

## II. MODIS LAI/FPAR Algorithm and Products

### A. Algorithm Inputs

The algorithm performs retrievals of LAI and FPAR from daily surface reflectance data at 1 km resolution. Currently, the

Manuscript received January 17, 2005; revised October 20, 2005. This work was supported by the NASA Earth Science Enterprise.

W. Yang, D. Huang, B. Tan, N. V. Shabanov, Y. Knyazikhin, and R. B. Myneni are with the Department of Geography, Boston University, Boston, MA 02215 USA (e-mail: ywze@crsa.bu.edu).

J. C. Stroeve is with the National Snow and Ice Data Center, University of Colorado, Boulder, CO 80309 USA.

R. R. Nemani is with the Ecosystem Science and Technology Branch, NASA Ames Research Center, Moffett Field, CA 94035 USA.

Digital Object Identifier 10.1109/TGRS.2006.871214

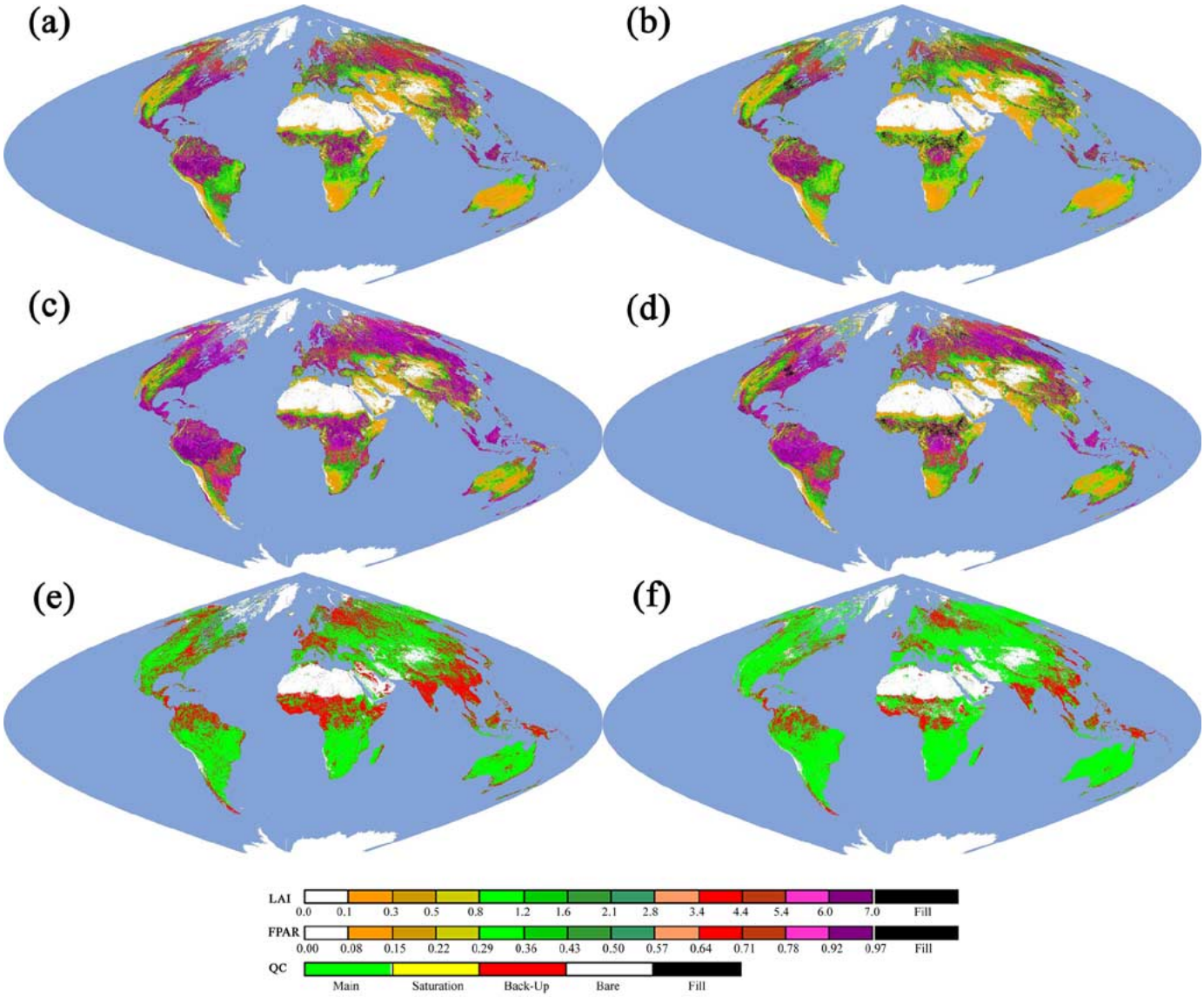


Fig. 1. Global maps of LAI, FPAR and Quality Control (QC) generated from Collection 3 (panels a, c, e) and Collection 4 (b, d, f) data sets for Julian dates 217–225 in year 2002 (August 5–13, 2002).

red (648 nm) and near-infrared (858 nm) bands are utilized because of high uncertainties in the other land bands [10]. Another important input to the algorithm is the biome classification map, in which the global vegetation is stratified into six canopy architectural types, or biomes [20]. The six biomes are: 1) grasses and cereal crops, 2) shrubs, 3) broadleaf crops, 4) savannas, 5) broadleaf forests, and 6) needle leaf forests. These biomes span structural variations along the horizontal (homogeneous versus heterogeneous) and vertical (single- versus multistory) dimensions, canopy height, leaf type, soil brightness, and climate (precipitation and temperature) space of herbaceous and woody vegetation. The biome map reduces the number of unknowns of the inverse problem through the use of simplifying assumptions (e.g., model leaf normal orientation distributions) and standard constants (e.g., leaf, wood, litter, and soil optical properties) that are assumed to vary with biome and soil types only. This approach is similar to that adopted in many global models which assume certain key parameters to vary only by vegetation type and utilize a land cover classification to achieve biome specific parameterization.

### *B. Algorithm*

The retrievals are performed with the radiative transfer algorithm, also called the main algorithm hereafter [4], [5]. The algorithm finds LAI and FPAR values given sun and view directions, Bidirectional Reflectance Factor (BRF) for each MODIS band, band uncertainties, and six biome land cover classes. The retrieval technique compares observed and modeled BRFs for a suite of canopy structures and soil patterns that represent an expected range of typical conditions for a given biome type. All canopy/soil patterns for which modeled and observed BRFs differ within a specified uncertainties level are considered as acceptable solutions. The mean values of LAI averaged over all acceptable solutions are reported as the output of the algorithm. This physically-based LAI and FPAR algorithm was developed

TABLE I
INTERPRETATION OF THE COLLECTION THREE QUALITY FLAGS ACCOMPANYING THE TERRA MODIS LAI AND FPAR PRODUCTS

| Variable | Bitfield, Bits | Binary, | Description of bitfield(s) |
|---|---|---|---|
| FparLai_QC | MODLAND {0,1} | 00=0 | Highest overall quality |
| | | 01=1 | Good quality |
| | | 10=2 | Not produced, cloud |
| | | 11=3 | Not able to produce |
| | ALGOR_PATH {2} | 0=0 | Empirical method used |
| | | 1=1 | R-T Main method used |
| | DEAD_ DETECTOR {3} | 0=0 | No dead detectors |
| | | 1=1 | Dead detector |
| | CLOUDSTATE {4,5} | 00=0 | Cloud free |
| | | 01=1 | Cloud covered pixel |
| | | 10=2 | Mixed clouds present |
| | | 11=3 | Not set, assume clear |
| | SCF_QC {6,7} | 00=0 | Best model result |
| | | 01=1 | Good quality, not the best |
| | | 10=2 | Use with caution, see other QA |
| | | 11=3 | Could not retrieve with either method |
| FparExtra_QC | LANDMASK {0,1} | 00=0 | Land (terrestrial class) |
| | | 01=1 | Shoreline, shallow water |
| | | 10=2 | Freshwater, inland lakes |
| | | 11=3 | Ocean |
| | SNOW_ICE {2} | 0=0 | No snow on pixel |
| | | 1=1 | Significant snow detected |
| | AEROSOL {3} | 0=0 | Low or no aerosol on pixel |
| | | 1=1 | Med or High aerosol on pixel |
| | CIRRUS {4} | 0=0 | No cirrus cloud detected |
| | | 1=1 | Cirrus clouds present |
| | ADJACENT-CLOUD {5} | 0=0 | No adjacent clouds detected |
| | | 1=1 | Adjacent clouds detected |
| | CLOUDSHADOW {6} | 0=0 | No cloud shadow detected |
| | | 1=1 | Cloud shadow was detected |
| | SCF_MASK {7} | 0=0 | User mask bit unset |
| | | 1=1 | User mask bit set |

for operational use with MODIS data. The main algorithm retrievals, therefore, are the MODIS standard product. The algorithm, however, may fail if input reflectance data uncertainties are greater than preset threshold values in the algorithm or due to deficiencies in model formulation which result in incorrect simulated BRFs. In all such cases, the retrievals are generated by a backup algorithm based on biome-specific empirical relationships between the Normalized Difference Vegetation Index (NDVI) and LAI/FPAR [21]. Additional details on algorithm physics can be found in [6], [7], [10], and [22].

### C. LAI and FPAR Products

The products are produced at 1-km spatial resolution daily and composited over an eight-day period based on the maximum FPAR value. The eight-day product is distributed to the public from the EROS Data Center Distributed Active Archive Center [WWW1]. Collection 3 represents the first significant processing of MODIS data into products after various initial problems with instrument calibration and electronics have been resolved, and covers the 26-month period from November 2000 to December 2002. This Collection, thus, provided an opportunity for evaluating the initial batch of products from Terra MODIS. These efforts lead to algorithm refinements which were implemented in Collection 4 processing that started in January 2003. Collection 4 represents the latest version of MODIS products and contains the entire time series of data starting from February 2000 to the present.

MODIS products are projected on the Integerized Sinusoidal (Collection 3) and the Sinusoidal (Collection 4) ten-degree grids, where the globe is tiled into 36 tiles along the east-west axis, and 18 tiles along the north-south axis [23]. Both Collection 3 and 4 MODIS LAI and FPAR products have been stage-1 validated [WWW2], that is, product accuracy has been estimated using a small number of independent measurements from selected locations and time periods through ground-truth and validation efforts [19].

The product files contain quality flags in addition to LAI and FPAR fields. The quality flag bit-fields provide information about the overall quality of the product, algorithm path, cloud state, aerosols, snow, etc. (Tables I and II). The users are advised to use the quality control variables to select reliable retrievals. Examples of global maps of LAI, FPAR and quality control variables for Collection 3 and 4 products are shown in Fig. 1 for composite days August 5–13, 2002.

### D. Changes in Collection Processing

The Collection 4 processing of LAI and FPAR products benefited from improved inputs (surface reflectance data and biome

TABLE II
INTERPRETATION OF THE COLLECTION FOUR QUALITY FLAGS ACCOMPANYING THE TERRA MODIS LAI AND FPAR PRODUCTS

| Variable | Bitfield, Bits | Binary, Decimal Values | Description of bitfield(s) |
|---|---|---|---|
| FparLai_QC | MODLAND {0,1} | 00=0 | Best possible |
| | | 01=1 | OK, but not the best |
| | | 10=2 | Not produced, due to cloud |
| | | 11=3 | Not produced, due to other reasons |
| | DEAD_ DETECTOR {2} | 0=0 | Detectors apparently fine for up to 50% of channels 1, 2 |
| | | 1=1 | Dead detectors caused >50% adjacent detector retrievals |
| | CLOUDSTATE {3,4} | 00=0 | Significant clouds NOT present (clear) |
| | | 01=1 | Significant clouds WERE present |
| | | 10=2 | Mixed clouds present on pixel |
| | | 11=3 | Cloud state not defined, assumed clear |
| | SCF_QC, {5,6,7} | 000=0 | Main (RT) method used with the best possible results |
| | | 001=1 | Main (RT) method used with saturation |
| | | 010=2 | Main (RT) method failed due to geometry problems, empirical method used |
| | | 011=3 | Main (RT) method failed due to problems other than geometry, empirical method used |
| | | 100=4 | Couldn't retrieve pixel |
| FparExtra_QC | LANDSEA {0,1} | 00=0 | Land |
| | | 01=1 | Shore |
| | | 10=2 | Freshwater |
| | | 11=3 | Ocean |
| | SNOW_ICE {2} | 0=0 | No snow, ice detected |
| | | 1=1 | Snow, ice were detected |
| | AEROSOL {3} | 0=0 | No or low atmospheric aerosol level detected |
| | | 1=1 | Average or high aerosol levels detected |
| | CIRRUS {4} | 0=0 | No cirrus cloud detected |
| | | 1=1 | Cirrus clouds present |
| | ADJACENT-CLOUD {5} | 0=0 | No clouds detected |
| | | 1=1 | Clouds WERE detected |
| | CLOUDSHADOW {6} | 0=0 | No cloud shadow detected |
| | | 1=1 | Cloud shadow was detected |
| | SCF_MASK {7,7} | 0=0 | Custom SCF mask, EXCLUDE this pixel |
| | | 1=1 | Custom SCF mask, INCLUDE this pixel |

map) and algorithm physics (LUTs and compositing), as discussed below. Refinements to atmospheric correction algorithm resulted in a significant increase in the spatial extent of high quality surface reflectance data. This directly impacted the spatial extent of the LAI and FPAR product (Fig. 1). The number of backup algorithm retrievals decreased from Collection 3 to 4, but this meant more main algorithm retrievals under saturation in broadleaf forests. The Advanced Very High-Resolution Radiometer (AVHRR) data-based biome map used in Collection 3 processing had high uncertainties compared to the MODIS data-based biome map used in Collection 4 [20]. The two maps are shown in Fig. 2 and compared in Table III. The Collection 3 biome map had significant misclassification of grasses and cereal crop pixels into broadleaf crop pixels which impacted LAI and FPAR retrievals. The quality of retrievals was especially low in the case of misclassification between forest and nonforest vegetation classes [8], [23].

The Collection 3 algorithm look-up tables (LUTs) were based on surface reflectance data from the Sea-Viewing Wide Field-of-view Sensor (SeaWiFS) sensor [10] while the Collection 4 LUTs were based on MODIS surface reflectance data. LAI histograms for the six biomes shown in Fig. 3 illustrate the impact of LUTs on LAI retrievals. The main problem with Collection 3 product was LAI overestimation in the first four biome types (Section II-A). This was also ascertained through validation activities [24], [19]. The problem was traced to mismatch between simulated reflectances evaluated from LUT entries and MODIS reflectances, thus resulting in incorrect LAI/FPAR retrievals or algorithm failure [11]. The LUTs were, therefore, revised according to the process described in [4], [8], and [9].

The compositing scheme of the algorithm was revised in Collection 4 processing. Amongst the set of LAI/FPAR values from the eight-day compositing period, the LAI/FPAR pair corresponding to the maximum FPAR value was selected, irrespective of algorithm path, to represent the eight-day composited MODIS LAI product in Collections 1–3. This scheme lead to poor quality compositing results when backup retrievals number more than the main algorithm retrievals in the eight-day period because the backup algorithm retrievals are inherently derived from lower quality inputs. This compositing scheme was changed in Collection 4 to select the LAI/FPAR pair corresponding to the maximum FPAR value generated by the main algorithm. The backup algorithm retrievals are selected only

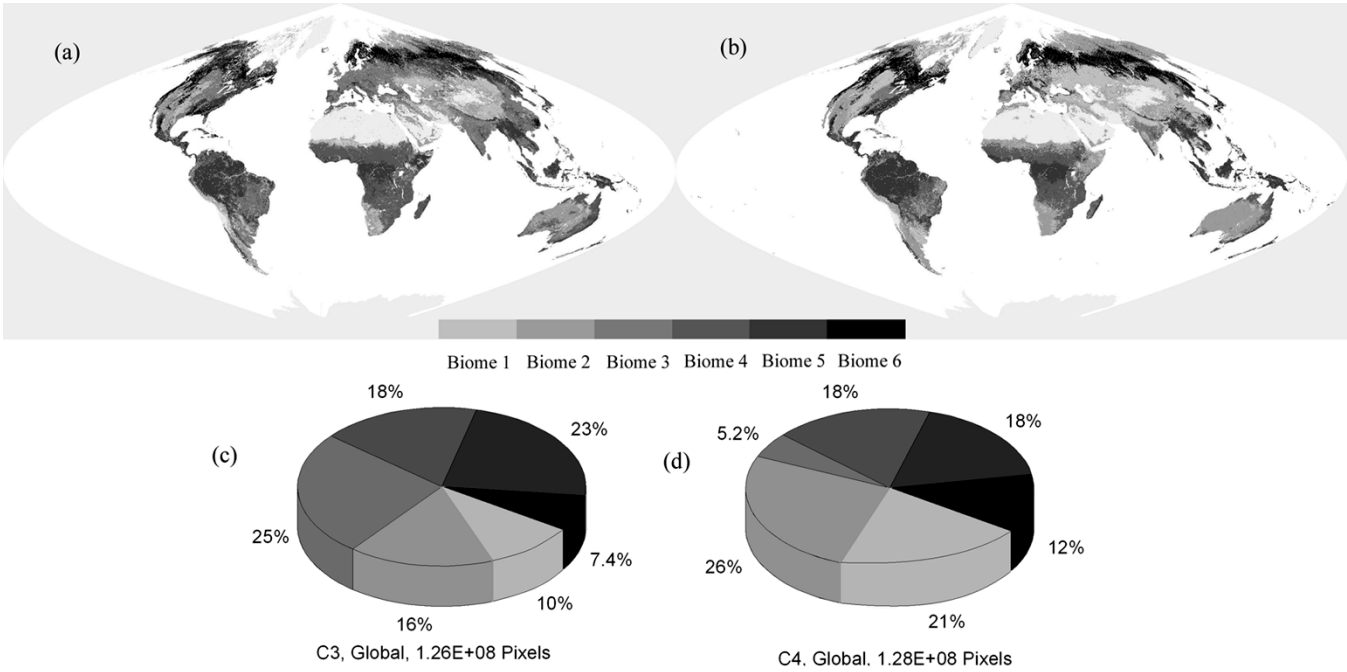


Fig. 2. Comparison of biome maps used in Collection 3 (panel a) and 4 (panel b) processing. The relative proportions are shown in panels c and d. A detailed comparison is presented in Table III.

TABLE III
ERROR MATIX FROM COMPARISON OF BIOME MAPS USED IN COLLECTIONS 3 AND 4 LAI/FPAR PROCESSING

| | | Collection 4 | | | | | | Grades | Commission |
|---|---|---|---|---|---|---|---|---|---|
| | | **1** | **2** | **3** | **4** | **5** | **6** | | |
| **Collection 3** | **1** | **6,971,916** | 4,322,864 | 49,112 | 601,569 | 294,292 | 156,694 | 12,396,447 | 0.44 |
| | **2** | 1,551,204 | **15,182,997** | 6,765 | 373,789 | 34,268 | 72,636 | 7,221,659 | 0.28 |
| | **3** | 15,199,428 | 1,581,210 | **5,904,694** | 3,711,853 | 3,383,863 | 1,594,219 | 31,875,267 | 0.81 |
| | **4** | 1,773,897 | 4,301,898 | 225,554 | **13,902,508** | 1,273,124 | 559,623 | 22,036,604 | 0.37 |
| | **5** | 825,483 | 3,211,906 | 295,052 | 2,949,431 | **16,119,732** | 4,877,476 | 28,279,080 | 0.43 |
| | **6** | 358,864 | 498,111 | 45,945 | 721,119 | 423,462 | **7,163,254** | 9,210,755 | 0.22 |
| **Grades** | | 26,680,792 | 19,098,986 | 6,527,122 | 22,260,269 | 22,028,741 | 14,423,902 | | |
| **Omission** | | 0.74 | 0.73 | 0.10 | 0.38 | 0.27 | 0.50 | | |

Total Samples: 111,019,812
Overall Accuracy: **49.8%**

when no main algorithm retrievals are available during the compositing period.

## III. RESULTS AND DISCUSSION

### A. Retrieval Index

The retrieval index (RI) is defined as the ratio of the number of pixels with LAI and FPAR retrieved by the main algorithm to the total number of retrievals by both the main and backup algorithms. This index does not indicate retrieval quality but rather the success rate of the main algorithm. The retrieval index shows a stable but seasonal pattern through the five years of MODIS operations [Fig. 4(a)]. The annual average retrieval index increased from 55% in Collection 3 to 67% in Collection 4 because of the changes discussed in Section II-D. The retrieval index can be as low as 40%–50% during the boreal winter time mainly due to poor quality surface reflectances and as high as 65%–80% during the boreal summer time. The points shown off the line in Fig. 4(a) are due to a pause in data collection by the Terra MODIS instrument [WWW3].

Grasses and cereal crops have the highest retrievals from the main algorithm (50% in winter and 80%–90% in summer) when retrievals are analyzed by biome type [Fig. 4(b)]. The retrieval rate is lowest in the case of broadleaf forests (40% through the year) because of reflectance saturation in dense canopies, that is, the reflectances do not contain sufficient information to localize a LAI value [4], [5]. Changes planned for Collection 5 processing are aimed at improving the retrieval rate in dense forests [9]. The seasonality in retrieval rate is most pronounced in the high northern latitudes [Fig. 4(c)]. The few main algorithm retrievals during the winter time in this region are due to snow and/or cloudy conditions and fewer measurements (surface reflectances are not generated for solar zenith angle $>70^{\circ}$). The retrieval index for this region is as high as 80% during the summer time. Overall, the retrieval rates of the main algorithm increased by 8%–16% in all latitudes in

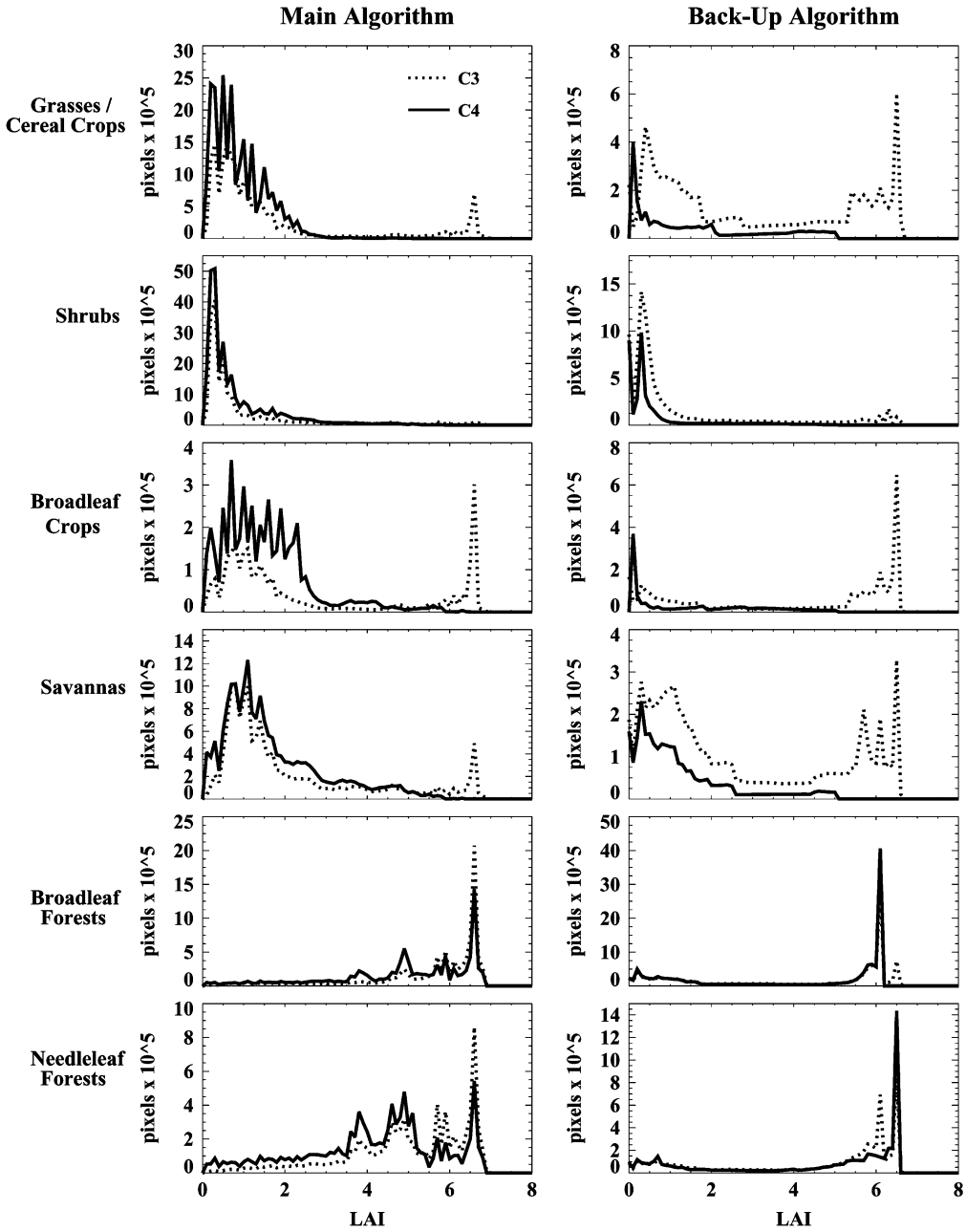


Fig. 3. LAI histograms from Collection 3 (dashed line) and 4 (solid line) by biome type and algorithm path.

the Collection 4 processing. Table IV summarizes the overall effect of version (Collection 3 versus 4) on LAI/FPAR retrievals from the main algorithm.

### *B. LAI and FPAR Fields*

The time series of LAI and FPAR fields from the Terra MODIS sensor exhibit the seasonal cycle as expected, with a boreal winter time minimum of about 1.5 (1.3) and a boreal summer time maximum of about 2.5 (1.8) for the Collection 3 (Collection 4) processing [Fig. 5(a) and (b)]. The difference between the two Collections is due to two reasons—1) LAI overestimation in the first four biomes (Section II-A) stemming from a mismatch between simulated reflectances evaluated from algorithm LUT entries and MODIS reflectances in Collection 3, and 2) significant misclassification of grasses and cereal crop pixels into broadleaf crop pixels in the biome map used in Collection 3 processing. The small random variations in the LAI time series are due to variations in data availability related to cloud cover rather than phenological changes. The global FPAR time series also shows similar seasonality, varying from about 0.45 in winter to 0.55 in summer. Thus, on average, about 50% of the incident photosynthetically active radiation is absorbed by vegetation. This high rate of absorption is possible because the vegetated area is magnified by a factor of 1.3 to 1.8 through layering of leaves in the canopy.

The LAI and FPAR profiles derived from the main algorithm for individual biomes are shown in Fig. 5(c) and (d). The amplitude of seasonal variations for a particular biome type at the global scale may be lower or different than the corresponding amplitude at regional scales. The Southern and Northern hemi-

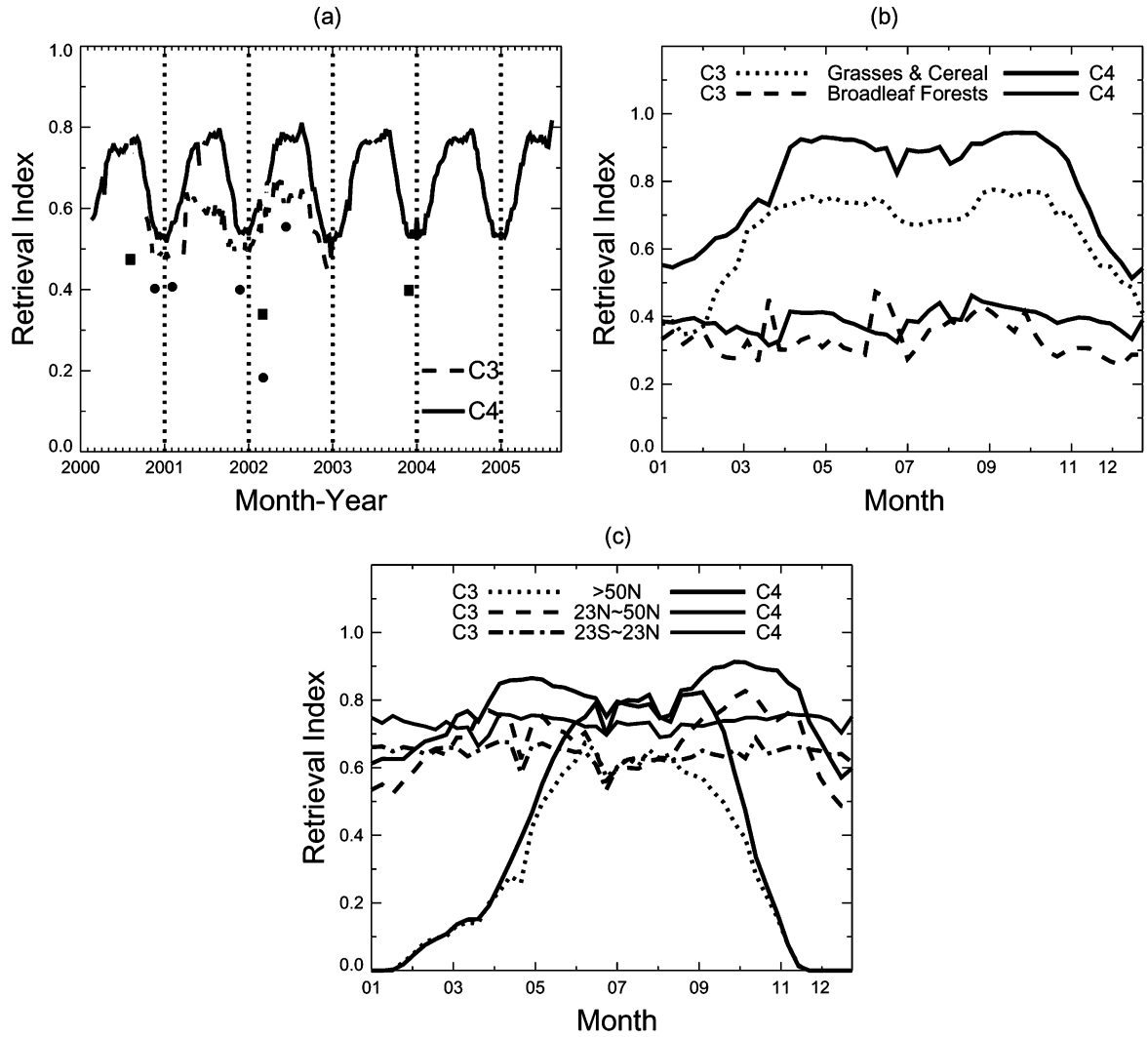


Fig. 4. Time series of the main algorithm retrieval rate, denoted here as the retrieval index (fraction of main algorithm retrievals) for Collection 3 (dashed lines) and 4 (solid lines) data sets. The global retrieval index is shown in panel a, the points shown off the line are due to a pause in data collection by the Terra MODIS instrument [WWW3]. The retrieval index for different biomes (latitudinal bands) is shown in panel b (panel c). The abbreviations C3 and C4 refer to Collection 3 and 4 products, respectively.

TABLE IV
TEMPORALLY AND SPATIALLY AVERAGED RETRIEVAL INDEX FOR SIX BIOMES IN COLLECTIONS 3 AND 4 LAI/FPAR PROCESSING

| | RI, % | | | | | |
|---|---|---|---|---|---|---|
| | Grasses and Cereal Crops | Shrubs | Broadleaf Crops | Savannas | Broadleaf Forests | Needleleaf Forests |
| **Collection 3** | 64 | 66 | 64 | 69 | 34 | 31 |
| **Collection 4** | 80 | 71 | 85 | 82 | 39 | 41 |

spheres have opposing growing seasons which dampen the seasonal amplitude at the global scale. Grasses and cereal crops have LAI values of about 1 through the year with negligible seasonal variations. Broadleaf forests indicate some seasonality with LAI varying from about 4 during the boreal winter to 5.5 in the summer. This biome class includes both evergreen broadleaf forests from the tropics and deciduous broadleaf forests from the temperate regions. A stronger seasonality is seen in needleleaf forests with LAI varying from about 2 during the boreal winter to 4.5 in the summer. Some of this seasonality is an artifact resulting from low data availability during the boreal winter time due to weak illumination conditions, extreme solar zenith angles, snow and cloud contamination.

The zonal mean LAI value from the tropics is about 1.5 in Collection 4 which may seem low [Fig. 5(e) and (f)]. In this band, large areas are under savanna (33%, LAI = 1.6), shrubs (17%, LAI = 0.6), and grasses (10%, LAI = 0.7). The evergreen broadleaf forests occupy 34% of the area in the tropics (23°S–23°N) with a mean LAI value of about 4.2. In the higher northern latitudes (>50°N), the summer time LAI values are about 2.5 in Collection 4. Low winter time LAI values here are an artifact due to snow and/or cloudy conditions, and the low availability of surface reflectances data. This will be further discussed in Sections III-D and III-E.

### C. Main and Backup Algorithm Retrievals

The foregoing analysis indicates that the main algorithm success rate is about 70% in Collection 4 processing. The main

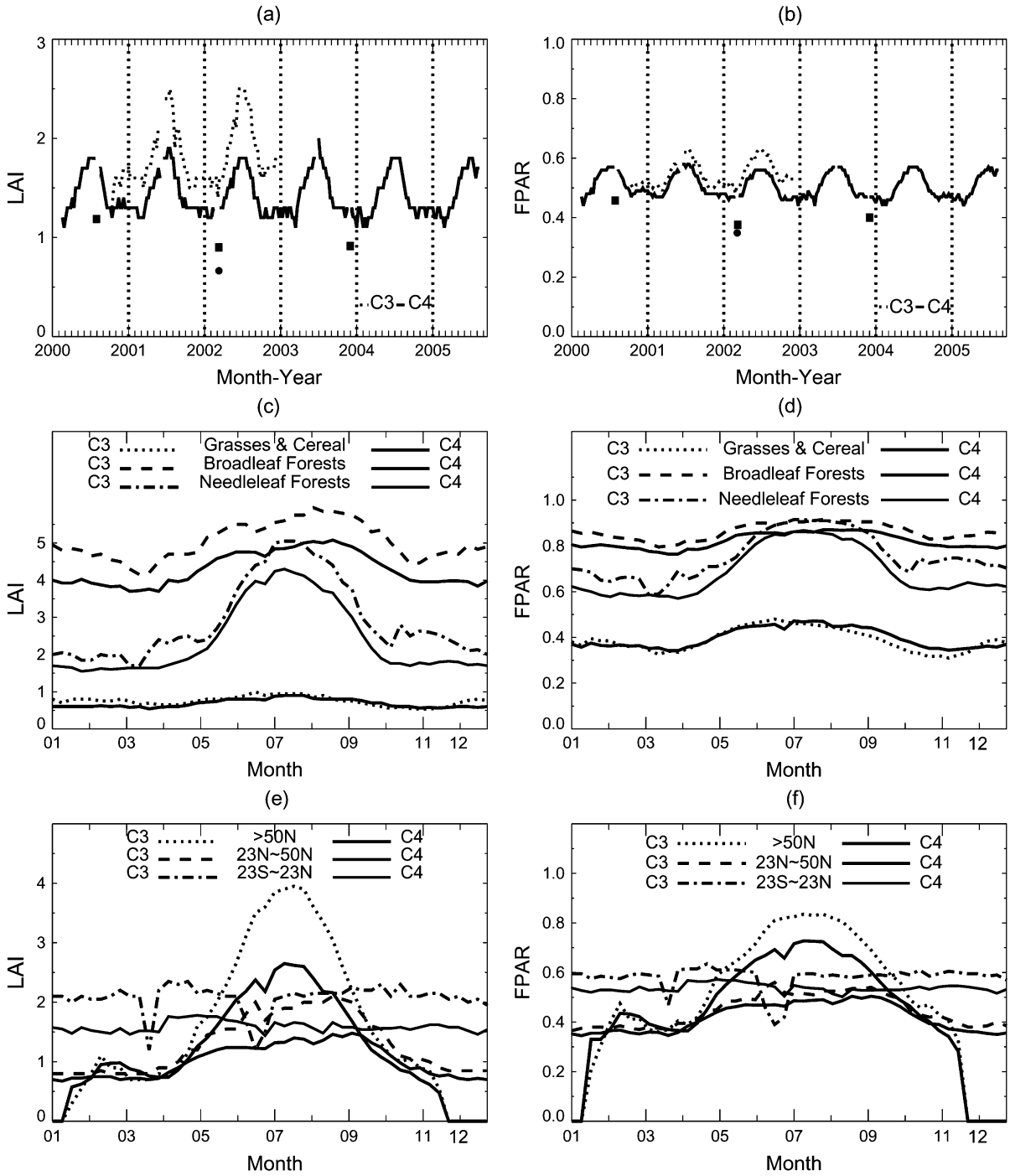


Fig. 5. LAI and FPAR from Collection 3 (dashed lines) and 4 (solid lines) data sets. The global retrieval index is shown in panels a and b. The averaged annual profile of LAI and FPAR for different biomes (latitudinal bands) is shown in panels c and d (panels e and f). The abbreviations C3 and C4 refer to Collection 3 and 4 products, respectively. (a) MOD15A2, Main Algorithm. (b) MOD15A2, Main Algorithm. (c) MOD15A2, Main Algorithm. (d) MOD15A2, Main Algorithm. (e) MOD15A2, Main Algorithm. (f) MOD15A2, Main Algorithm.

algorithm failure in 30% of the pixels may be due to uncertainties in input surface reflectance data greater than threshold values preset in the algorithm, biome misclassifications and algorithm deficiencies that can result in an incorrect or no match between simulated reflectances evaluated from LUT entries and MODIS reflectances. The backup NDVI based algorithm triggered in these instances is insensitive to input data uncertainties and always provides a retrieval if NDVI is a positive number. The quality of retrievals from the backup algorithm is, thus, generally poor. The following analysis was performed to compare main and backup algorithm retrievals.

The difference between the main and backup algorithms retrievals is defined as delta LAI (delta FPAR). Delta LAI is calculated at a monthly scale as a function of both biome type and latitudinal band. The four successive eight-day LAI values of a pixel in one month are flagged for further analysis if this sequence contains retrievals from both the main and backup algorithms. The mean main algorithm LAI, $\overline{\mathrm{LAI}}_{\mathrm{main}}$, and the mean

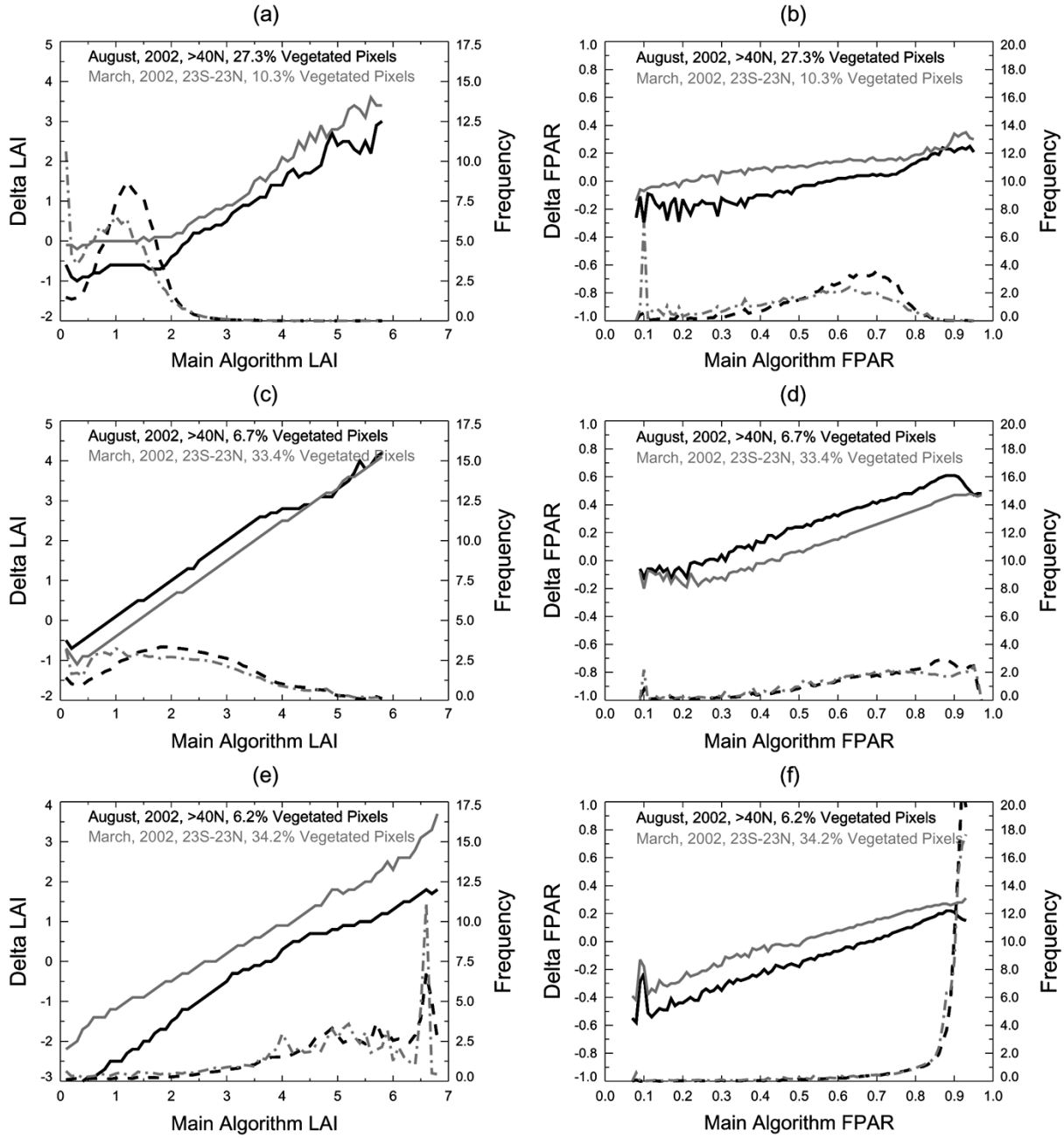


Fig. 6. Difference between main and backup algorithm retrievals in Collection 4 (solid lines). Results are shown for three representative biomes (grasses and cereal crops, savannas, and broadleaf forests), two-month (August and March) and two-latitudinal bands (north of 40°N and 23°S to 23°N). Also shown are the histograms of LAI and FPAR values retrieved by the main algorithm (dotted lines). (a) Grasses and Cereal Crops. (b) Grasses and Cereal Crops. (c) Savannas. (d) Savannas. (e) Broadleaf Forests. (f) Broadleaf Forests.

backup algorithm LAI, $\overline{\mathrm{LAI}}_{\mathrm{backup}}$, are used to evaluate delta LAI of the pixel, $\Delta\mathrm{LAI}_{\mathrm{pixel}} = \overline{\mathrm{LAI}}_{\mathrm{main}} - \overline{\mathrm{LAI}}_{\mathrm{backup}}$. Similar calculations are performed for FPAR data.

Representative delta LAI and FPAR fields evaluated with the Collection 4 data are shown in Fig. 6 for three biome types (grasses and cereal crops, savannas, and broadleaf forests) in two broad latitude bands (north of 40°N and 23°S–23°N) during two representative months (August and March). Delta LAI and FPAR are generally linear with respect to the mean main algorithm LAI and FPAR values. Delta FPAR is less than 0.2 in two of the three biomes studied (Fig. 6) over the range of the most probable FPAR values (0.4–0.8 in grasses and cereal crops and 0.8–0.9 for broadleaf forests). However, delta FPAR is significantly higher (about 0.4) in savannas, where the most probable FPAR values range from 0.6 to 0.95. The same is true of delta LAI. Grasses and cereal crops have a low LAI values (0.5–2.0) and delta LAI is close to zero for a majority of pixels. Broadleaf forests have high LAI values (4.0–6.5) and delta LAI is also high—about 1.8 in the northern latitudes during August and 3.4 in the tropical band during March.

The above-mentioned differences in LAI and FPAR values from the main and backup algorithms highlight certain limitations of the backup algorithm. Recall that the backup algorithm is based on biome-specific relations between NDVI and LAI (FPAR). These relations, although based on field data and model calculations, are, nevertheless, site-specific and can not account

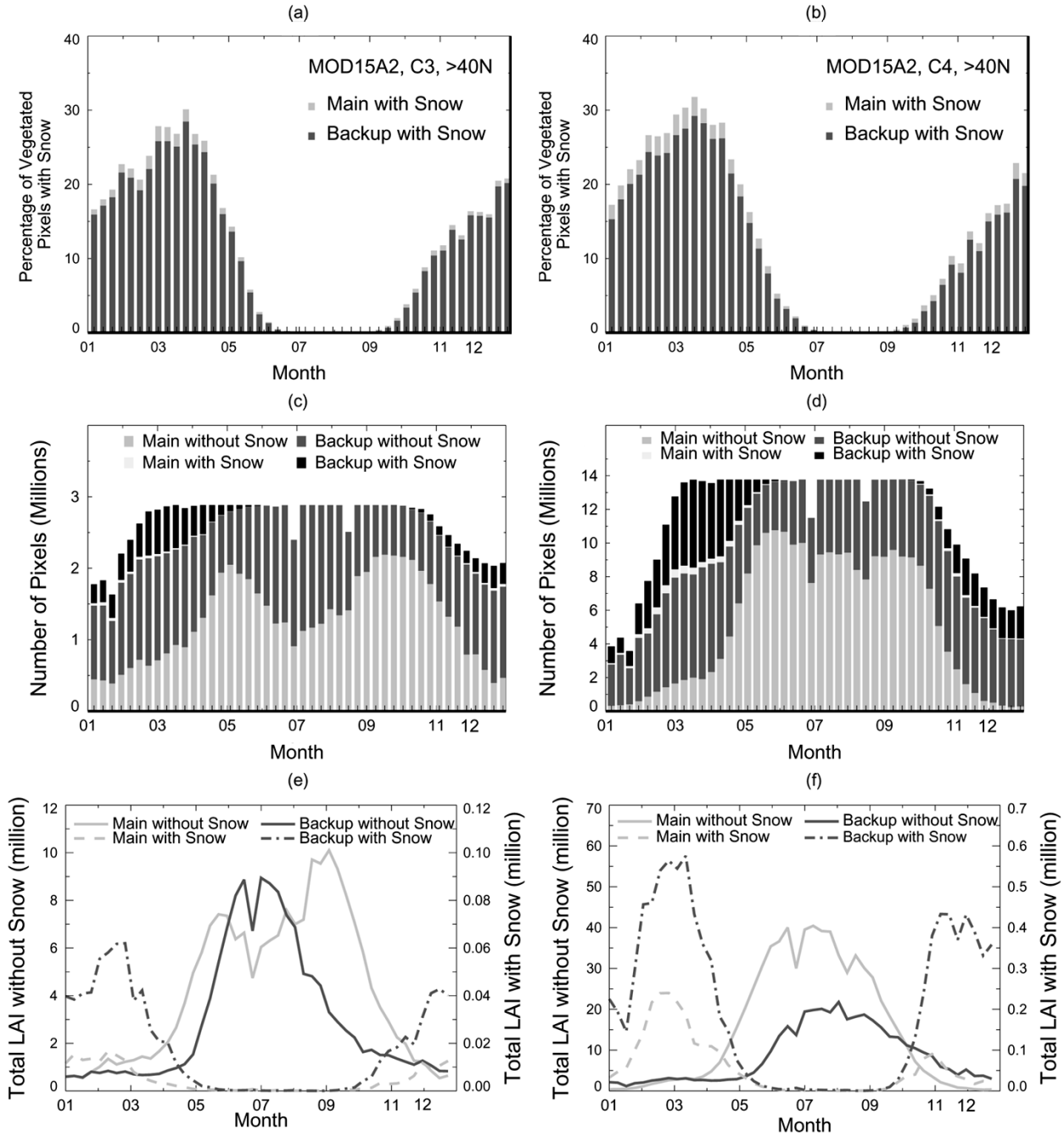


Fig. 7. Impact of snow on LAI/FPAR retrievals over vegetated areas north of 40° N. The annual course of the percentage of snow covered pixels in Collection 3 (panel a) and 4 (panel b) data. The annual course of the pixel counts and total LAI (the sum of LAIs over corresponding pixels) retrieved by the Collection 4 main and backup algorithms under various snow conditions is shown for broadleaf forests (panels c and e) and needleleaf forests (panels d and f). The abbreviations C3 and C4 refer to Collection 3 and 4 products, respectively.

for natural variability of vegetation. Moreover, an important reason why the main algorithm fails is cloud and snow contamination of surface reflectances. The backup algorithm will retrieve low LAI and FPAR values as it is insensitive to input uncertainties (Sections III-D and III-E). This analysis highlights the need for examining the product quality flags accompanying the product (Tables I and II).

### *D. Retrievals From Pixels With Snow*

The impact of snow cover on algorithm performance is examined here to understand the seasonality observed in LAI and FPAR fields in the boreal zones [Fig. 5(e) and (f)]. Information on snow cover of each pixel is contained in the product quality flags accompanying the products (Tables I and II). According to this information, about 20% to 30% of the vegetated pixels north of 40°N are identified as having snow during the peak winter months [Fig. 7(a) and (b)]. Under such conditions, the main algorithm retrieval rate is 1.4% in Collection 3 and 2.5% in Collection 4. The high failure rate is due to the fact that snow significantly increases both RED and NIR reflectances, such that NDVI is close to 0 [25], and the reflectances are not part of the retrieval domain of the main algorithm. The backup

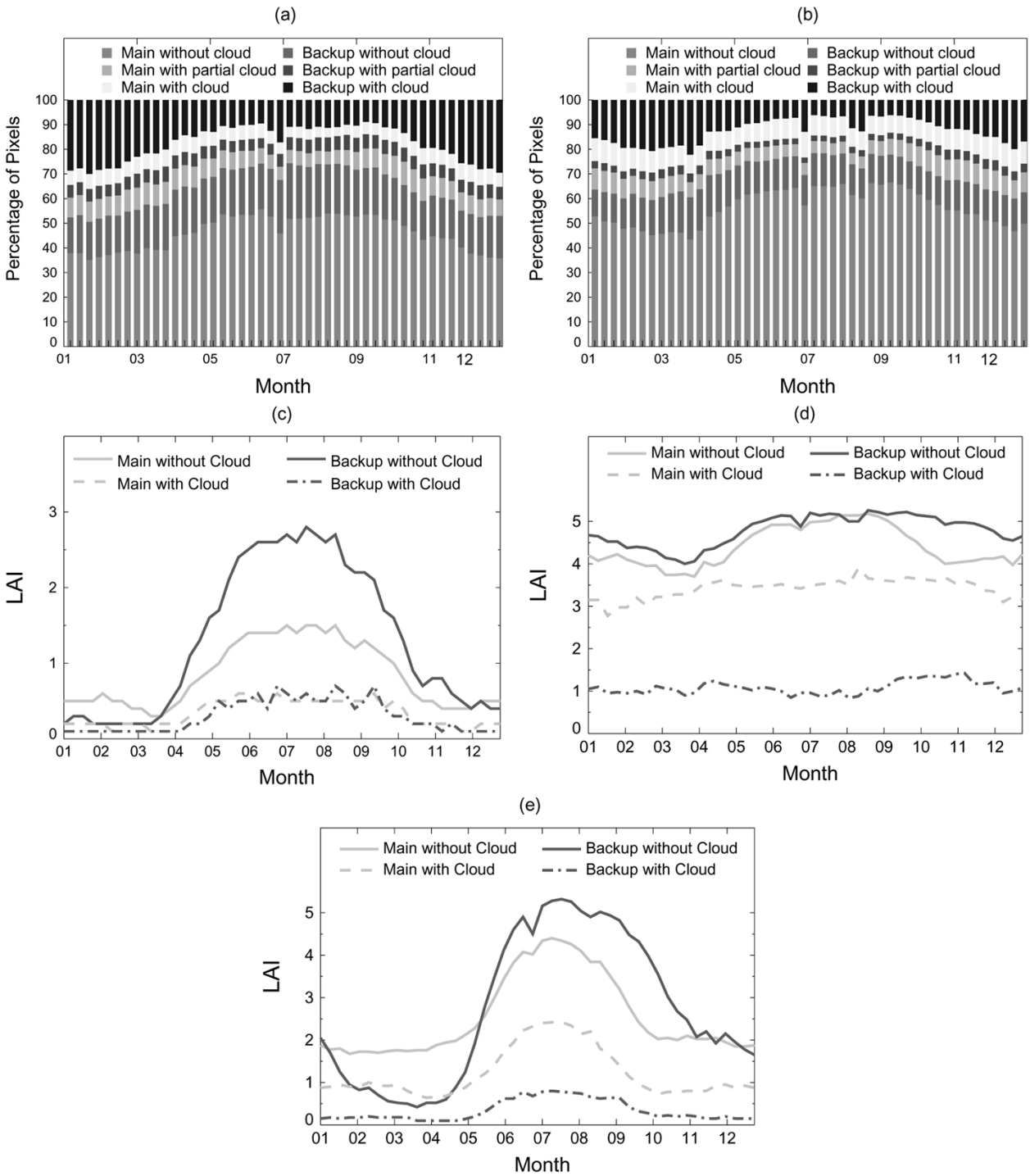


Fig. 8. Impact of clouds on LAI/FPAR retrievals. Three cloud conditions were used—cloudy, partially cloudy, and clear. The annual course of the percentage of pixels retrieved by the main or the backup algorithms under various cloud conditions in Collection 3 (panel a) and 4 (panel b) data. The annual course of LAI retrieved by the Collection 4 main and backup algorithms under different cloud conditions is shown in panel c for grasses and cereal crops, in panel d for broadleaf forests and in panel e for needleleaf forests. (a) Collection 3. (b) Collection 4. (c) Grasses and Cereal Crops. 25.4% Vegetated Pixels, Northern Hemisphere. (d) Droadleaf Forests, 17.7% Vegetated, Pixels, Global. (e) Needleleaf Forests, 12.0% Vegetated Pixels, Global.

NDVI-based algorithm invoked in these cases provides LAI and FPAR retrievals close to 0. Such pixels are tagged as having poor quality in the QA fields (Tables I and II).

The Collection 4 LAI retrievals under various snow conditions in the high northern latitudes ($>40^{\circ}$N) are shown in Fig. 7(c)–(f), separately for broadleaf and needleleaf forests. Total LAI (the sum of LAI values over corresponding pixels), instead of average LAI, is shown in Fig. 7(e) and (f). The total LAI under snow-free conditions is about 100 times greater than that with snow, that is, LAI retrievals under snow conditions are a very small portion of the total retrievals, generally speaking. During the winter months, however, retrievals under snow conditions are considerable, and, in fact, there are too few main algorithm retrievals to reliably estimate average LAI values

for needleleaf forest pixels [Fig. 7(d)]. Therefore, the LAI and FPAR seasonality in needleleaf forests, seen in Fig. 5(c)–(d), is spurious and must be treated as an artifact resulting from too few reliable retrievals. It should also be noted that there are few reliable measurements in the high northern latitudes during the winter period because of low sun angles and weak illumination conditions, which further amplify the problem of reliably estimating LAI and FPAR in these regions during the winter months.

### *E. Retrievals Under Cloudy Conditions*

The MODIS cloud screening algorithm uses as many as 14 of the MODIS 36 spectral bands to maximize the reliability of cloud detection. Information on cloud optical thickness, effective radius, cloud-top properties is also used to determine the cloud mask (e.g., single layer, multilayer, clear sky, etc.). Details on the MODIS cloud mask are described in [26].

Information on pixel cloud state is contained in quality flags accompanying the products (Tables I and II). Note that the LAI/FPAR algorithm is executed irrespective of cloud state. About 50% to 65% of the vegetated pixels are identified as cloud free, 15% as partially cloudy and the rest as cloud covered in the Collection 3 data set [Fig. 8(a)]. In Collection 4, about 65% to 75% of the vegetated pixels are identified as cloud free, 10% as partially cloudy and the rest as cloud covered [Fig. 8(b)]. These differences must be attributed to refinements in cloud screening algorithm. The increase in the amount of cloud free pixels in Collection 4 is especially noticeable during the boreal winter time period [Fig. 8(a) and (b)].

The annual course of Collection 4 LAI retrieved by the main and backup algorithms under different cloud conditions is shown in Fig. 8(c)–(e) for three example biomes (grasses and cereal crops, broadleaf forests, and needleleaf forests). The majority of retrievals under cloudy conditions are performed with the backup algorithm. Main algorithm failure in such cases is expected as the input reflectance data have large uncertainties. The main algorithm does not fail in some limited cases of cloudiness [cf. Fig. 8(b)]. This situation may correspond to the case of cloud cover overestimation by the cloud screening algorithm. The results shown in Fig. 8 suggest that the annual course of LAI values retrieved by the main algorithm shows similar patterns, irrespective of the degree of cloudiness. However, the differences in LAI magnitudes between the retrievals under cloud-free and cloudy conditions are not negligible, and they depend on the biome type and the time of the year. This again reinforces the need for examining the product quality flags accompanying the LAI and FPAR product (Tables I and II).

## IV. Conclusion

The following conclusions can be drawn based on the analysis of two years of Collection 3 and five years of Collection 4 Terra MODIS LAI and FPAR data sets. The success rate of the main radiative transfer algorithm increased from 55% in Collection 3 to 67% in Collection 4. This is due to the new LUTs implemented in Collection 4 and also due to refinements to upstream algorithms that provide inputs to the LAI/FPAR algorithm. The time series of LAI and FPAR fields exhibit the seasonal cycle with a boreal winter time minimum of about 1.5 (1.3) and a boreal summer time maximum of about 2.5 (1.8) for the Collection 3 (Collection 4) processing. This difference between the two Collections is due to two reasons—1) LAI overestimation in the first four biomes (Section II-A) stemming from a mismatch between simulated reflectances evaluated from algorithm LUT entries and measured MODIS reflectances in Collection 3, and 2) significant misclassification of grasses and cereal crop pixels into broadleaf crop pixels in the biome map used in Collection 3 processing. Less than 2%–3% of the pixels tagged as covered with snow are processed by the main algorithm. Thus, most of the snow covered pixels are processed by the backup NDVI-based algorithm which is insensitive to input reflectance data quality. Similarly, a majority of retrievals under cloudy conditions are obtained from the backup algorithm. For these reasons, the backup algorithm retrievals have low quality and should not be used for validation and other studies. The users are advised to consult the quality flags accompanying the LAI and FPAR product to select high quality retrievals.

The analysis presented here demonstrates the physical basis of the main algorithm used to generate the MODIS standard LAI and FPAR product, and importantly, that the reliability and spatial coverage of the retrievals increase with increased input accuracy. Further improvements in the quality of MODIS surface reflectances and biome map are, therefore, expected to lead to LAI and FPAR product of increasing quality and coverage. The role of the backup algorithm will be consequently reduced.

## Appendix I
## WWW Sites

WWW1: EROS Data Center Distributed Active Archive Center, http://edcimswww.cr.usgs.gov/pub/imswelcome/ WWW2: The EOS Land Validation Home Page, http://landval.gsfc.nasa.gov/ WWW3: Terra MODIS Instrument Performance History, http://www.mcst.ssai.biz/mcstweb/performance/terra_instrument.html.

## Acknowledgment

The authors would like to thank the many individuals who contributed to the successful and timely operational processing of MODIS data, especially Dr. El Saleous, Dr. Friedl, Dr. Justice, Dr. Roy, Dr. Vermote, and and Dr. Wolfe for their effort and support.

## References

[1] W. L. Barnes, T. S. Pagano, and V. V. Salomonson, "Prelaunch characteristics of the moderate resolution imaging spectroradiometer (MODIS) on EOS-AM1," *IEEE Trans. Geosci. Remote Sens.*, vol. 36, no. 4, pp. 1088–1100, Jul. 1998.

[2] C. O. Justice, J. R. G. Townshend, E. F. Vermote, E. Masuoka, R. E. Wolfe, N. Saleous, D. P. Roy, and J. T. Morisette, "An overview of MODIS land data processing and product status," *Remote Sens. Environ.*, vol. 83, pp. 3–15, 2002.

[3] P. J. Sellers, R. E. Dickinson, D. A. Randall, A. K. Betts, F. G. Hall, J. A. Berry, G. J. Collatz, A. S. Denning, H. A. Mooney, C. A. Nobre, N. Sato, C. B. Field, and A. Henderson-Sellers, "Modeling the exchanges of energy, water, and carbon between continents and the atmosphere," *Science*, vol. 275, pp. 502–509, 1997.

[4] Y. Knyazikhin, J. V. Martonchik, R. B. Myneni, D. J. Diner, and S. W. Running, "Synergistic algorithm for estimating vegetation canopy leaf area index and fraction of absorbed photosynthetically active radiation from MODIS and MISR data," *J. Geophys. Res.*, vol. 103, pp. 32 257–32 274, 1998.

[5] Y. Knyazikhin, J. V. Martonchik, D. J. Diner, R. B. Myneni, M. Verstraete, B. Pinty, and N. Gobron, "Estimation of vegetation leaf area index and fraction of absorbed photosynthetically active radiation from atmosphere-corrected MISR data," *J. Geophys. Res.*, vol. 103, pp. 32 239–32 256, 1998.

[6] O. Panferov, Y. Knyazikhin, R. B. Myneni, J. Szarzynski, S. Engwald, K. G. Schnitzler, and G. Gravenhorst, "The role of canopy structure in the spectral variation of transmission and absorption of solar radiation in vegetation canopies," *IEEE Trans. Geosci. Remote Sens.*, vol. 39, no. 2, pp. 241–253, Feb. 2001.

[7] Y. Tian, Y. Wang, Y. Zhang, Y. Knyazikhin, J. Bogaert, and R. B. Myneni, "Radiative transfer based scaling of LAI/FPAR retrievals from reflectance data of different resolutions," *Remote Sens. Environ.*, vol. 84, pp. 143–159, 2002.

[8] Y. Tian, Y. Zhang, Y. Knyazikhin, R. B. Myneni, J. M. Glassy, G. Dedieu, and S. W. Running, "Prototyping of MODIS LAI and FPAR algorithm with LASUR and LANDSAT data," *IEEE Trans. Geosci. Remote Sens.*, vol. 38, no. 5, pp. 2387–2401, Sep. 2000.

[9] N. V. Shabanov, S. Kotchenova, D. Huang, W. Yang, Y. Knyazikhin, and R. B. Myneni, "Optimization of the MODIS LAI and FPAR algorithm performance over broadleaf forests," *IEEE Trans. Geosci. Remote Sens.*, vol. 43, no. 8, pp. 1835–1865, Aug. 2005.

[10] Y. Wang, Y. Tian, Y. Zhang, N. El-Saleous, Y. Knyazikhin, E. Vermote, and R. B. Myneni, "Investigation of product accuracy as a function of input and model uncertainities: Case study with SeaWiFS and MODIS LAI/FPAR algorithm," *Remote Sens. Environ.*, vol. 78, pp. 296–311, 2001.

[11] B. Tan, D. Huang, J. Hu, W. Yang, P. Zhang, N. V. Shanabov, Y. Knyazikhin, and R. B. Myneni, "Assessment of the broadleaf crops leaf area index product from the terra MODIS instrument," *Agric. Forest Meteorol.*, vol. 135, pp. 124–134, Sep. 2005.

[12] J. T. Morisette, J. L. Privette, and C. O. Justice, "A framework for the validation of MODIS land products," *Remote Sens. Environ.*, vol. 83, pp. 77–96, 2002.

[13] J. L. Privette, R. B. Myneni, Y. Knyazikhin, M. Mukufute, G. Roberts, Y. Tian, Y. Wang, and S. G. Leblanc, "Early spatial and temporal validation of MODIS LAI product in africa," *Remote Sens. Environ.*, vol. 83, pp. 232–243, 2002.

[14] N. V. Shabanov, Y. Wang, W. Buermann, J. Dong, S. Hoffman, G. R. Smith, Y. Tian, Y. Knyazikhin, and R. B. Myneni, "Effect of foliage spatial heterogeneity in the MODIS LAI and FPAR algorithm over broadleaf forests," *Remote Sens. Environ.*, vol. 85, pp. 410–423, 2003.

[15] Y. Tian, C. E. Woodcock, Y. Wang, J. L. Privette, N. V. Shabanov, L. Zhou, Y. Zhang, W. Buermann, J. Dong, B. Veikkanen, T. Hame, K. Anderson, M. Ozdogan, Y. Knyazikhin, and R. B. Myneni, "Multiscale analysis and validation of the MODIS LAI product. I. Uncertainty assessment," *Remote Sens. Environ.*, vol. 83, pp. 414–430, 2002.

[16] ——, "Multiscale analysis and validation of the MODIS LAI product. II. Sampling strategy," *Remote Sens. Environ.*, vol. 83, pp. 431–441, 2002.

[17] Y. Wang, C. E. Woodcock, W. Buermann, P. Stenberg, P. Voipio, H. Smolander, T. Hame, Y. Tian, J. Hu, Y. Knyazikhin, and R. B. Myneni, "Evaluation of the MODIS LAI algorithm at a coniferous forest site in Finland," *Remote Sens. Environ.*, vol. 91, pp. 114–127, 2004.

[18] B. Tan, J. Hu, P. Zhang, D. Huang, N. V. Shabanov, M. Weiss, Y. Knyazikhin, and R. B. Myneni, "Validation of MODIS LAI product in croplands of Alpilles, France," *J. Geophys. Res.*, vol. 110, p. D01107, 2005. 10.1029/2004JD004 860.

[19] W. Yang, B. Tan, D. Huang, M. Rautiainen, N. V. Shabanov, Y. Wang, J. L. Privette, K. F. Huemmrich, R. Fensholt, I. Sandholt, M. Weiss, R. R. Nemani, Y. Knyazikhin, and R. B. Myneni, "MODIS leaf area index products: From validation to algorithm improvement," *IEEE Trans. Geosci. Remote Sens.*, vol. 44, no. 7, pp. 1885–1898, Jul. 2006.

[20] M. A. Friedl, D. K. McIver, J. C. F. Hodges, X. Y. Zhang, D. Muchoney, A. H. Strahler, C. E. Woodcock, S. Gopal, A. Schneider, and A. Cooper, "Global land cover mapping from MODIS: Algorithms and early results," *Remote Sens. Environ.*, vol. 183, pp. 287–302, 2002.

[21] R. B. Myneni, R. R. Nemani, and S. W. Running, "Estimation of global leaf area index and absorbed par using radiative transfer models," *IEEE Trans. Geosci. Remote Sens.*, vol. 35, no. 6, pp. 1380–1393, Nov. 1997.

[22] N. V. Shabanov, Y. Knyazikhin, F. Baret, and R. B. Myneni, "Stochastic modeling of radiation regime in discontinuous vegetation canopies," *Remote Sens. Environ.*, vol. 74, pp. 125–144, 2000.

[23] R. B. Myneni, S. Hoffman, Y. Knyazikhin, J. L. Privette, J. Glassy, Y. Tian, Y. Wang, X. Song, Y. Zhang, G. R. Smith, A. Lotsch, M. Friedl, J. T. Morisette, P. Votava, R. R. Nemani, and S. W. Running, "Global products of vegetation leaf area and fraction absorbed PAR from year one of MODIS data," *Remote Sens. Environ.*, vol. 83, pp. 214–231, 2002.

[24] W. B. Cohen, T. K. Maiersperger, Z. Yang, S. T. Gower, D. P. Turner, W. D. Ritts, M. Berterretche, and S. W. Running, "Comparisons of land cover and LAI estimates derived from ETM+ and MODIS for four sites in North America: A quality assessment of 2000/2001 provisional MODIS products," *Remote Sens. Environ.*, vol. 88, pp. 233–255, 2003.

[25] D. K. Hall, G. A. Riggs, V. V. Salomonson, N. E. DiGirolamo, and K. J. Bayr, "MODIS snow-cover products," *Remote Sens. Environ.*, vol. 83, pp. 181–194, 2002.

[26] S. A. Ackerman, K. I. Strabala, P. W. P. Menzel, R. A. Frey, C. C. Moeller, and L. E. Gumley, "Discriminating clear sky from clouds with MODIS," *J. Geophys. Res.*, vol. 103, no. D24, pp. 32 141–32 157, 1998.

**Wenze Yang** received the B.S. and M.S. degrees in automation from Tsinghua University, Beijing, China, in 2001, respectively, and the Ph.D. degree from Boston University, Boston, MA, in 2006.

His research interests focus on the remote sensing of vegetation, the diagnosis and evaluation of satellite-retrieved surface data, and climate–vegetation interactions.

**Dong Huang** received the B.S. degree in physics from Beijing Normal University, Beijing, China, in 1999. He is currently pursuing the Ph.D. degree at Boston University, Boston, MA.

His research is focused on radiative transfer modeling in vegetation canopies with emphasis on parameterization of 3-D effects.

**Bin Tan** received the Ph.D. degree in geography from Boston University, Boston, MA, in 2005.

He is currently a Postdoctoral Research Associate in the Department of Geography, Boston University, where he is working on MODIS land cover and phenology products. His research interests are in remote sensing of vegetation.

**Julienne C. Stroeve** received the B.S. and M.S. degrees in aerospace engineering and the Ph.D. degree in geography from the University of Colorado, Boulder, in 1989, 1991, and 1996, respectively. Her Ph.D. thesis dealt with deriving a radiation climatology of the Greenland ice sheet using satellite imagery.

She has been a Research Scientist with the National Snow and Ice Data Center, University of Colorado since 1996. Her research interests include optical, thermal and microwave remote sensing of snow- and ice-covered surfaces, cryosphere–climate interactions, atmospheric radiative transfer modeling, and image processing.

**Nikolay V. Shabanov** received the M.A. degree in physics from Moscow State University, Moscow, Russia, and the Ph.D. degree in remote sensing from Boston University, Boston, MA, in 1996 and 2002, respectively.

He is currently a Research Assistant Professor with the Geography Department, Boston University. His scientific interests includes parameterization of the effect of vegetation spatial heterogeneity with stochastic radiative transfer theory, BRDF modeling, development of the algorithms for retrievals of vegetation biophysical parameters from satellite data, satellite data fusion, and assimilation of satellite data in land climate models. Dr. Shabanov has been a research leader for NASA's MODIS LAI/FPAR project during last 3.5 years.

**Yuri Knyazikhin** received the M.S. degree in applied mathematics from Tartu University, Tartu, Estonia, and the Ph.D. degree in numerical analysis from the N. I. Muskhelishvilli Institute of Computing Mathematics, the Georgian Academy of Sciences, Tbilisi, Georgia, in 1978 and 1985, respectively.

He was a Research Scientists at the Institute of Astrophysics and Atmospheric Physics and Tartu University, Computer Center of the Siberian Branch of the Russian Academy of Sciences, from 1978 to 1990. He was an Alexander von Humboldt Fellow from 1990 to 1996. He is currently a Research Professor in the Department of Geography, Boston University, Boston, MA. He has worked and published in areas of numerical integral and differential equations, theory of radiative transfer in atmospheres and plant canopies, remote sensing of the atmosphere and plant canopies, ground-based radiation measurements, forest ecosystem dynamics, and modeling multifunctional forest management.

**Ramakrishna R. Nemani**, photograph and biography not available at the time of publication.

**Ranga B. Myneni** received the Ph.D. degree in biology from the University of Antwerp, Antwerp, Belgium, in 1985.

Since then, he has been with Kansas State University, Manhattan, the University of Gottingen, Gottingen, Germany, and the NASA Goddard Space Flight Center, Greenbelt, MD. He is currently a Professor and Member of the Faculty at the Department of Geography, Boston University, Boston, MA. His research interests are in radiative transfer, remote sensing of vegetation, and climate–vegetation dynamics. He is a MODIS and MISR Science Team Member.